Technical Summary

Performance Analysis of the OBB-TM Algorithm for Lidar-based Pose Estimation of Non-Cooperative Space Targets

Giuliano Pennacchio

1. Introduction

On-Orbit Servicing (OOS) and Active Debris Removal (ADR) missions rely critically on robust relative navigation capabilities to enable safe rendezvous, inspection, capture, and manipulation of resident space objects. A fundamental requirement in these operations is the estimation of the full six-degree-of-freedom (6-DoF) relative pose—position and attitude—of a target spacecraft. The problem becomes significantly more challenging when the target is non-cooperative, i.e., not equipped with dedicated navigation aids such as retro-reflectors, fiducial markers, or communication support.

In non-cooperative scenarios, the relative navigation chain typically consists of two distinct phases: (i) pose acquisition (lost-in-space condition), where no prior information on the target orientation is assumed, and (ii) tracking, where the pose estimate is continuously refined once a valid initialization has been established. The acquisition phase is particularly critical, as it must resolve the global orientation of the target under severe sensing and geometric constraints.

LiDAR sensors are well suited for this task due to their capability to provide direct three-dimensional range measurements in the form of point clouds. Nevertheless, long-range LiDAR-based acquisition introduces several technical challenges, including:

- Sparse and non-uniform point cloud sampling,
- Partial field-of-view (FOV) coverage,
- Centroid bias due to incomplete geometry observation,
- Structural symmetries inducing pose ambiguities,
- Limited computational resources for onboard implementation.

To address these challenges, this work investigates the performance of the OBB-TM (Oriented Bounding Box – Template Matching) algorithm for LiDAR-based pose acquisition of non-cooperative spacecraft. The method combines principal component analysis (PCA) for canonical frame alignment, a one-degree-of-freedom (1-DoF) template database for coarse attitude initialization, and Iterative Closest Point (ICP) refinement, optionally augmented by an ambiguity reduction strategy for symmetric geometries.

The objective of this study is to characterize the robustness, accuracy, and operational envelope of the OBB-TM pipeline under varying sensing conditions. The algorithm is evaluated through a systematic simulation campaign involving multiple spacecraft geometries with different symmetry properties, a wide range of distances, and different LiDAR angular resolutions. Performance is assessed using quantitative success metrics based on translational and rotational estimation errors.

2. Problem Formulation

2.1 Pose Acquisition in Lost-in-Space Conditions

The problem addressed in this work is the estimation of the relative 6-DoF pose of a non-cooperative target spacecraft using LiDAR point cloud measurements, in the absence of prior orientation information. The target is assumed to be observed from distances ranging from tens to over one hundred meters, where point cloud sparsity and partial visibility effects become significant.

Let F_C denote the chaser reference frame and F_T the target body-fixed frame. The objective is to estimate the rigid transformation $(\mathbf{R},\mathbf{t}) \in SE(3)$ such that:

- $\mathbf{R} \in SO(3)$ represents the rotation matrix from F_T to F_C,
- $\mathbf{t} \in \mathbb{R}^3$ represents the relative translation vector expressed in F_C.

The available measurement is a LiDAR point cloud $P = \{p_i\}_{i=1}^{N}$, expressed in the chaser frame. A CAD model of the target geometry is assumed to be known a priori and serves as the reference model for registration.

The pose acquisition problem can therefore be formulated as a model-to-scan registration task under the following constraints:

- No initial attitude guess (global orientation unknown),
- Sparse and partially observed surface points,
- Possible geometric symmetries,
- No feature markers or semantic cues.

2.2 Challenges of Long-Range LiDAR Registration

At large distances, the angular resolution of the LiDAR sensor directly affects the spatial density of the measured point cloud. As distance increases, the sampling becomes increasingly sparse, leading to:

- Reduced geometric constraints,
- Increased sensitivity to noise,
- Degraded convergence properties of local registration algorithms such as ICP.

Moreover, partial FOV coverage introduces centroid bias and incomplete surface representation. In symmetric spacecraft geometries, different attitude configurations may produce similar point cloud structures, leading to ambiguous registration solutions.

These aspects make direct application of local optimization methods insufficient for global pose acquisition. A coarse initialization strategy capable of reducing the solution space prior to local refinement is therefore required.

2.3 Performance Metrics

To evaluate the effectiveness of the pose acquisition pipeline, a success-based performance metric is adopted. For each Monte Carlo simulation case, the estimated pose $(\widehat{\boldsymbol{R}}, \widehat{\boldsymbol{t}})$ is compared to the ground truth $(\mathbf{R}_{gt}, \mathbf{t}_{gt})$.

A trial is considered successful if both of the following conditions are satisfied:

- Translational error:

$$\|\hat{\boldsymbol{t}} - \boldsymbol{t}_{gt}\| < 0.2\ m$$

- Rotational error:

$$\theta\left(\widehat{\boldsymbol{R}}\boldsymbol{R}_{gt}^{T}\right) < 5°$$

where $\theta(\cdot)$ denotes the principal rotation angle associated with the rotation matrix.

The primary performance indicator used in this study is the Success Rate (SR), defined as the percentage of successful trials over the total number of Monte Carlo runs for a given distance and sensor resolution.

This formulation enables quantitative assessment of the algorithm robustness across different operational conditions and spacecraft geometries.

3. OBB-TM Pose Acquisition Algorithm

The OBB-TM (Oriented Bounding Box – Template Matching) algorithm is designed to address the global pose acquisition problem under sparse and partial LiDAR observations. The method combines a geometry-based canonical alignment strategy with a reduced-dimensional template search and local refinement.

The overall pipeline consists of the following stages:

1) PCA-based canonical frame extraction and OBB construction
2) 1-DoF template database generation (offline)
3) Template matching for coarse attitude estimation
4) ICP-based fine registration
5) Optional ambiguity reduction for symmetric targets

Each stage is described in detail in the following subsections.

3.1 PCA-Based Canonical Alignment and Oriented Bounding Box (OBB)

A key challenge in global pose acquisition is the absence of an initial attitude guess. Direct application of local registration methods such as ICP may fail due to convergence to local minima. To reduce the search space dimensionality, the OBB-TM method first computes a canonical reference frame through Principal Component Analysis (PCA).

Given a point cloud $P = \{p_i\}_{i=1}^{N}$, the centroid is computed as:

$$\bar{\boldsymbol{p}} = \frac{1}{N}\sum_{i=1}^{N} \boldsymbol{p}_i$$

The covariance matrix is then defined as:

$$\boldsymbol{C} = \frac{1}{N}\sum_{i=1}^{N} (\boldsymbol{p}_i - \bar{\boldsymbol{p}})(\boldsymbol{p}_i - \bar{\boldsymbol{p}})^T$$

Eigen-decomposition of $\boldsymbol{C}$ provides three orthogonal principal axes corresponding to the directions of maximum variance. These axes define a canonical frame in which the point cloud is approximately aligned with its principal geometric directions.

Oriented Bounding Box (OBB)

Using the PCA frame, an Oriented Bounding Box (OBB) is constructed around the target model. Unlike an axis-aligned bounding box (AABB), the OBB is aligned with the principal axes of the geometry, enabling:

- Compact geometric representation,
- Consistent canonical orientation,
- Reduction of rotational ambiguity.

The OBB serves two main purposes:

1) It defines the principal axis about which the residual rotational degree of freedom is parameterized.
2) It provides a structured way to generate rotated model templates for coarse matching.

While PCA significantly reduces the orientation search space, it does not fully determine the rotation around the dominant principal axis. This residual degree of freedom motivates the introduction of a one-dimensional template search.

3.2 One-Degree-of-Freedom Template Database

After canonical alignment, the pose estimation problem is reduced to resolving a single rotational degree of freedom around the dominant principal axis.

Offline Template Generation

An offline database of model templates is generated by rotating the known CAD model around the selected principal axis over a discrete set of angles:

$$\theta_k = k\Delta\theta, \;\; k = 0,1,\ldots,K-1$$

where Δθ is the angular resolution of the template database.

For each angle θ_k, a rotated version of the model point cloud is stored. This precomputation significantly reduces onboard computational burden during acquisition.

Online Template Matching

During operation, the PCA-aligned LiDAR point cloud is compared against each template in the database. For each candidate template, a registration score is computed, typically based on the residual error after preliminary alignment.

The template producing the minimum residual is selected as the coarse pose estimate:

$$\theta^* = argmin_{\theta_k} J(\vartheta_k)$$

where $J(\theta_k)$ denotes the alignment cost metric.

This procedure converts the global orientation search into a structured one-dimensional discrete optimization problem, improving robustness compared to blind ICP initialization.

3.3 ICP-Based Fine Registration

Following coarse initialization via template matching, the estimated pose is refined using the Iterative Closest Point (ICP) algorithm.

Given:

- Model point set M,
- Measured point cloud P,

ICP iteratively solves:

$$(\boldsymbol{R}, \boldsymbol{t}) = argmin_{\boldsymbol{R},\boldsymbol{t}} \sum_{i=1}^{N} \|\boldsymbol{p}_i - (\boldsymbol{R}\boldsymbol{m}_i + \boldsymbol{t})\|$$

Where m_i are corresponding points selected through nearest-neighbor association.

The coarse estimate provided by the template matching stage ensures that ICP initialization lies within the basin of attraction of the correct solution, significantly increasing convergence reliability under sparse sampling conditions. The refinement stage improves both translational and rotational accuracy and provides the residual metric used for ambiguity evaluation.

3.4 Ambiguity Reduction (AR) for Symmetric Targets

Spacecraft geometries often exhibit structural symmetries (e.g., rotational symmetry about a principal axis). In such cases, different orientations may produce similar LiDAR projections, leading to ambiguous pose solutions.

For example, a 180° rotation around a symmetry axis may yield a point cloud that is nearly indistinguishable under sparse sampling.

To mitigate this issue, an Ambiguity Reduction (AR) strategy is introduced.

Hypothesis Evaluation

After obtaining the nominal solution ($\mathbf{R}_1$, $\mathbf{t}_1$), an alternative symmetric hypothesis is constructed:

$$\boldsymbol{R}_2=\boldsymbol{R}_1\boldsymbol{R}_\pi$$

where $\boldsymbol{R}_\pi$ represents a 180° rotation around the symmetry axis.

Both hypotheses are refined using ICP and evaluated using their respective residual errors: J_1, J_2.

The final pose estimate is selected as:

$$(\boldsymbol{R},\boldsymbol{t}) = f(x) = \begin{cases}(\boldsymbol{R_1},\boldsymbol{t_1}), & if\ J_1 < J_2)\\ (\boldsymbol{R_2},\boldsymbol{t_2}), & otherwise\end{cases}$$

Impact on Performance

The AR module enhances robustness in the presence of geometric symmetries, particularly for targets exhibiting near-axis symmetry. Its effectiveness depends on:

- Point cloud density,
- Sensor resolution,
- Distance to target,
- Degree of geometric symmetry.

For strongly asymmetric targets, AR has limited impact, whereas for symmetric geometries it significantly improves the probability of correct global orientation recovery

Concluding Remarks on the Algorithm

The OBB-TM pipeline provides a structured solution to the lost-in-space LiDAR pose acquisition problem by:

- Reducing the 3-DoF rotational search to a 1-DoF discrete optimization,
- Leveraging geometric canonical alignment through PCA and OBB,
- Combining global coarse matching with local refinement,
- Explicitly addressing symmetry-induced ambiguities.

This hybrid approach balances computational tractability and robustness under sparse and partially observed measurement conditions, making it suitable for long-range non-cooperative spacecraft pose acquisition scenarios.

4. Simulation Campaign and Experimental Setup

To assess the robustness and operational envelope of the OBB-TM algorithm, a systematic simulation campaign was conducted. The objective was to evaluate the algorithm performance under varying geometric configurations, sensor resolutions, and target distances, representative of long-range acquisition phases in OOS and ADR missions.

The simulation framework reproduces realistic LiDAR sensing conditions and enables statistical performance assessment through Monte Carlo trials.

4.1 Target Models

Three representative spacecraft geometries were selected to investigate the influence of structural symmetry on pose acquisition performance:

- Envisat — asymmetric geometry
- TDRS — rotational symmetry around the Y-axis
- Dawn — rotational symmetry around the X-axis

These targets were chosen to span different symmetry characteristics:

- A largely asymmetric spacecraft (Envisat), expected to provide strong geometric constraints,
- A moderately symmetric spacecraft (TDRS),
- A configuration exhibiting pronounced symmetry properties (Dawn).

For each model, a high-fidelity CAD representation was used as the reference geometry for template generation and registration.

The inclusion of multiple symmetry classes enables evaluation of the Ambiguity Reduction (AR) module effectiveness under different structural conditions.

4.2 LiDAR Sensor Model

The LiDAR sensor was modeled as an ideal scanning device providing three-dimensional point measurements in the chaser reference frame.

The key parameters varied in the campaign were:

- Distance to target: 20 m to 120 m
- Angular resolution: 0.1°, 0.2°, 0.5°, 1.0°

Angular resolution directly determines spatial sampling density. As the target distance increases, the same angular resolution results in larger spatial separation between points, producing sparser point clouds.

No artificial feature markers or reflectivity enhancements were introduced, ensuring a strictly non-cooperative scenario.

Point clouds were generated considering:

- Line-of-sight visibility,
- Field-of-view constraints,
- Self-occlusion effects.

This modeling approach reproduces partial surface coverage and centroid bias phenomena typical of long-range acquisition.

4.3 Monte Carlo Campaign

To ensure statistical relevance, a Monte Carlo approach was adopted.

For each combination of:

- Target model,
- Distance,
- Angular resolution,

multiple randomized attitude configurations were generated. These random orientations simulate the lost-in-space condition, where the target orientation is completely unknown a priori.

Each simulation trial followed the full OBB-TM pipeline:

1. PCA alignment and OBB construction
2. 1-DoF template matching
3. ICP refinement
4. Optional Ambiguity Reduction

The resulting pose estimate was compared to ground truth to determine success or failure according to the criteria defined in Section 2.

This approach enables estimation of the Success Rate (SR) as a function of distance and resolution.

4.4 Success Criteria and Performance Indicators

Performance evaluation was based on a binary success metric defined by combined translational and rotational thresholds:

- Translational error < 0.2 m
- Rotational error < 5°

A trial is considered successful only if both criteria are satisfied.

For each configuration, the Success Rate (SR) is computed as:

$$SR = \frac{N_{success}}{N_{total}} \times 100\%$$

where:

- $N_{success}$ is the number of successful trials,
- N_{total} is the total number of Monte Carlo runs.

This metric provides a clear representation of the algorithm operational envelope and allows comparison across targets and sensing conditions.

4.5 Experimental Variables and Analysis Dimensions

The campaign investigates the following dependencies:

1. Distance sensitivity: degradation of performance with increasing range due to sparsity effects.
2. Angular resolution impact: influence of sensor resolution on geometric constraint richness.
3. Symmetry-induced ambiguity: performance difference between asymmetric and symmetric targets.
4. Effectiveness of Ambiguity Reduction (AR): comparison of SR with and without AR module.

This multidimensional evaluation enables identification of:

- Saturation regimes (high SR across distances),
- Transition regimes (performance sensitive to resolution),
- Failure regimes (significant SR degradation).

4.6 Computational Considerations

Although the study focuses on algorithmic performance, computational tractability remains an important aspect for onboard applicability.

The design choices of the OBB-TM pipeline contribute to computational efficiency:

- PCA reduces global search dimensionality,
- Template database is generated offline,
- 1-DoF discrete search limits runtime complexity,
- ICP is initialized within a constrained solution basin.

The simulation framework allows assessment of algorithm scalability across increasing template resolution and point cloud sparsity conditions.

5. Results and Performance Analysis

This section presents the performance evaluation of the OBB-TM pose acquisition algorithm across all simulated configurations. Results are first discussed from a global perspective to highlight general trends, and subsequently analyzed on a per-target basis to investigate geometry-dependent behavior.

5.1 Global Performance Trends

Across all targets and sensor configurations, the Success Rate (SR) exhibits a consistent dependency on both distance and angular resolution.

5.1.1 Influence of Distance

As expected, performance degrades with increasing distance. The primary cause is the reduction in spatial sampling density resulting from fixed angular resolution. Sparse point clouds:

- weaken geometric constraints,
- increase ICP sensitivity to local minima,
- amplify centroid bias under partial visibility.

At short to medium ranges, fine angular resolutions (0.1°–0.2°) generally yield near-saturation SR values, whereas coarser resolutions (0.5°–1.0°) show a sharper degradation beyond intermediate distances.

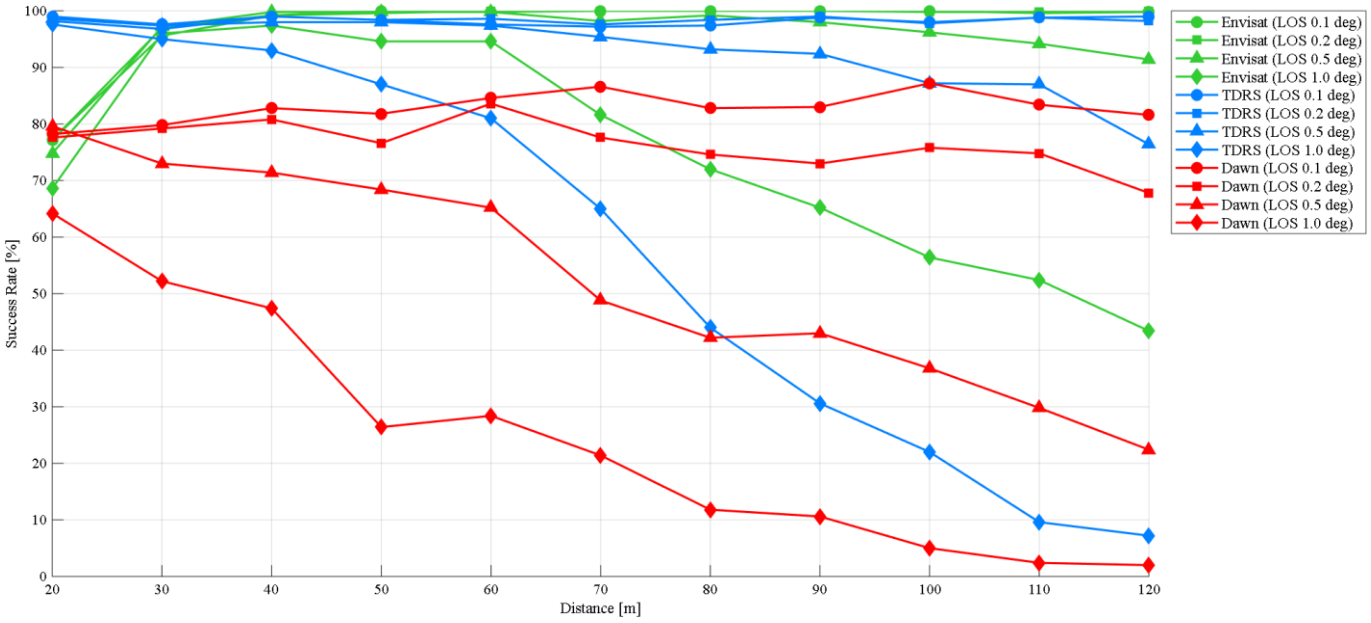

Figure 5.1 – SR vs Distance for all targets at all tested sensor resolutions (no AR)

The transition from high-SR regime to degradation regime defines the effective operational envelope of the algorithm.

5.1.2 Influence of Angular Resolution

Angular resolution directly controls point cloud density. The results confirm a nonlinear sensitivity:

- Fine resolutions maintain high SR across larger distances.
- Intermediate resolutions exhibit threshold behavior.
- Coarse resolutions significantly reduce acquisition reliability at long range.

This behavior highlights the strong coupling between sensing geometry and global registration stability.

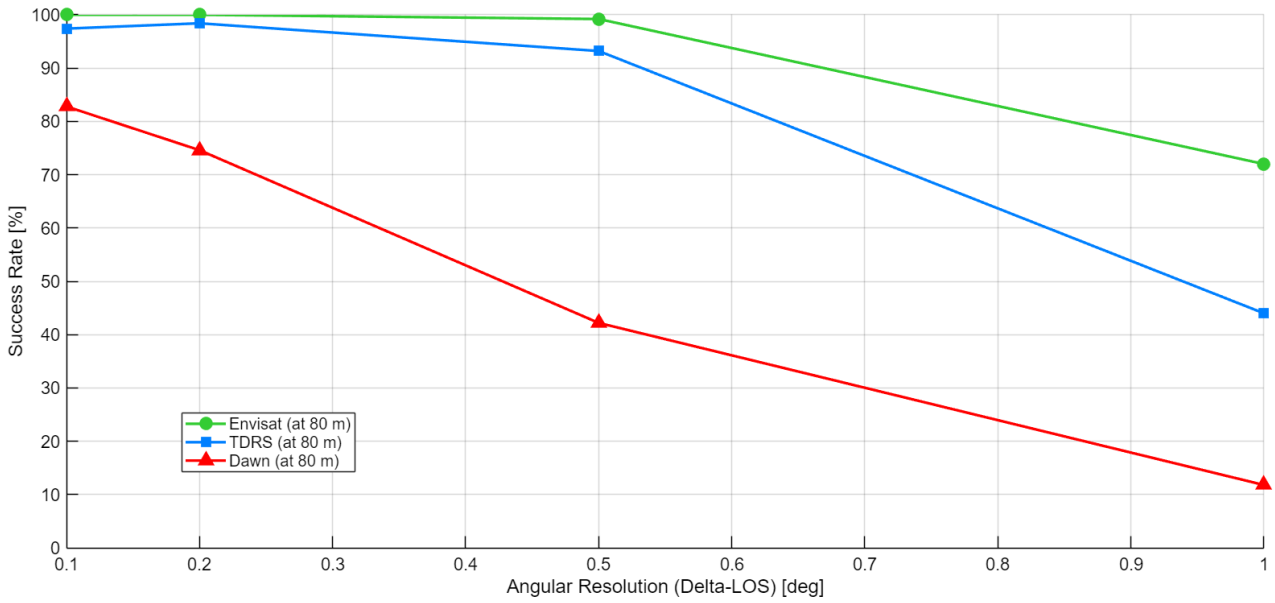

Figura 5.2 – SR vs Sensor Resolution at fixed distance (80m)

5.1.3 Effect of Ambiguity Reduction (AR)

The Ambiguity Reduction module shows target-dependent impact. Globally:

- Minimal effect for strongly asymmetric geometries,
- Moderate to significant improvement for symmetric targets,
- Greater benefit in mid-resolution regimes.

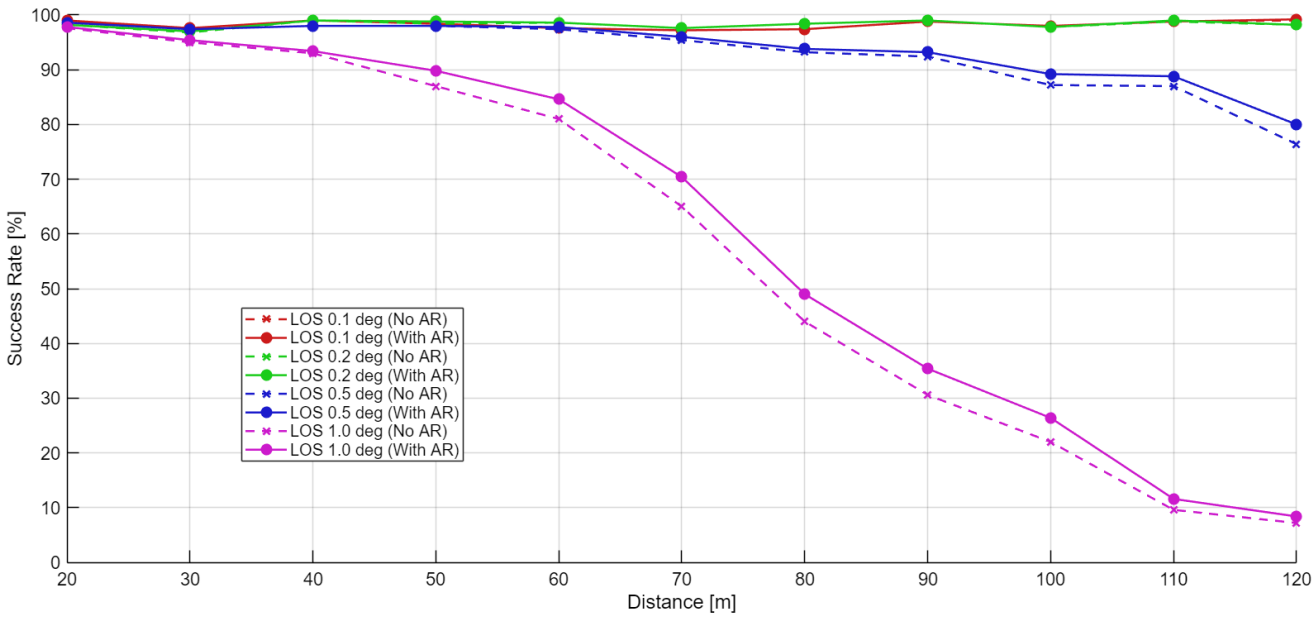

Figure 5.3 – SR comparison with/without AR -TDRS target all sensor Resolutions

The AR module primarily increases robustness in scenarios where symmetry-induced pose duplication is likely under sparse sampling.

5.2 Target-Specific Analysis

While global trends are consistent, geometric properties introduce important differences in performance behavior.

5.2.1 Envisat (Asymmetric Geometry)

Envisat represents the most geometrically asymmetric target in the campaign. As expected, it achieves the highest baseline Success Rate across configurations.

At fine resolutions (0.1°–0.2°), SR remains close to saturation even at extended ranges. Performance degradation becomes noticeable primarily at coarse resolution combined with long distance.

Interestingly, short-range anomalies are observed in specific configurations. These are attributable to:

- Partial FOV effects,
- Local centroid bias,
- Increased sensitivity to certain roll-pitch configurations.

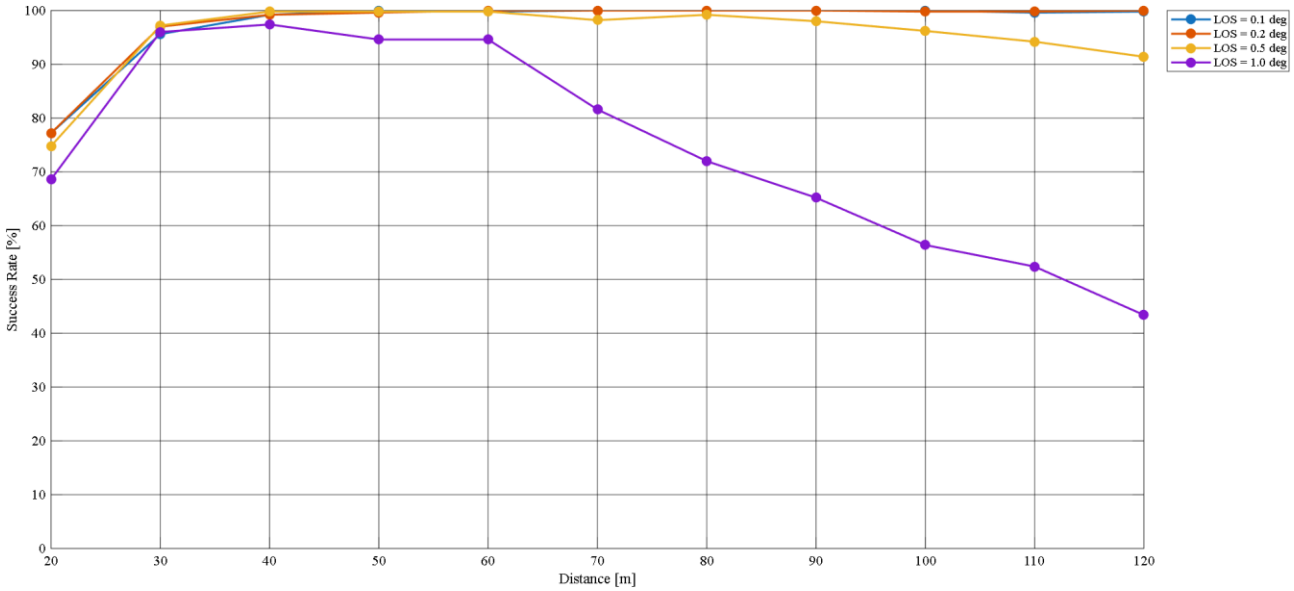

Figura 5.4 – SR vs Distance at all resolutions for Envisat

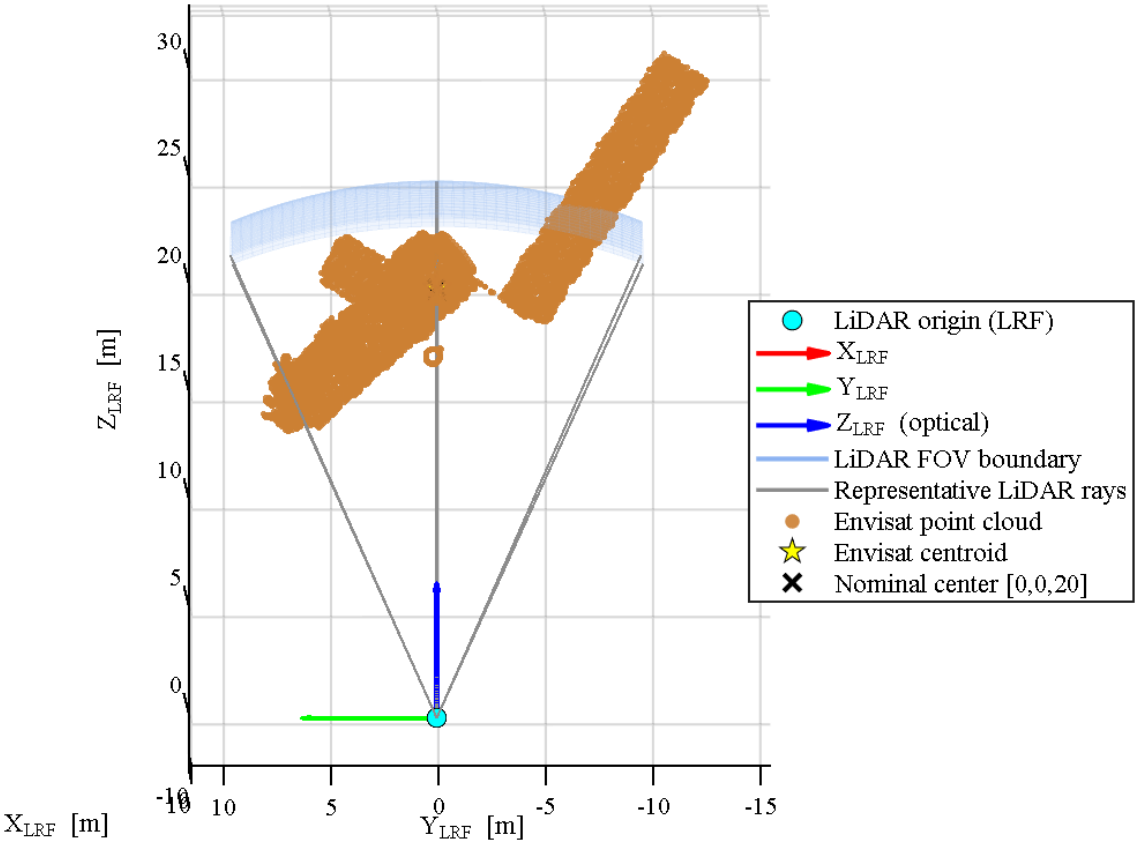

Figura 5.5 – Envisat at 20m from Lidar Sensor

The limited impact of the AR module confirms that symmetry-induced ambiguity is not a dominant factor for this geometry.

5.2.2 TDRS (Y-Axis Symmetry)

TDRS exhibits rotational symmetry about the Y-axis, introducing potential 180° ambiguity scenarios.

Without Ambiguity Reduction, SR degradation is observed in intermediate-to-coarse resolution regimes. The AR module provides measurable improvement by correctly resolving symmetric pose hypotheses through residual comparison.

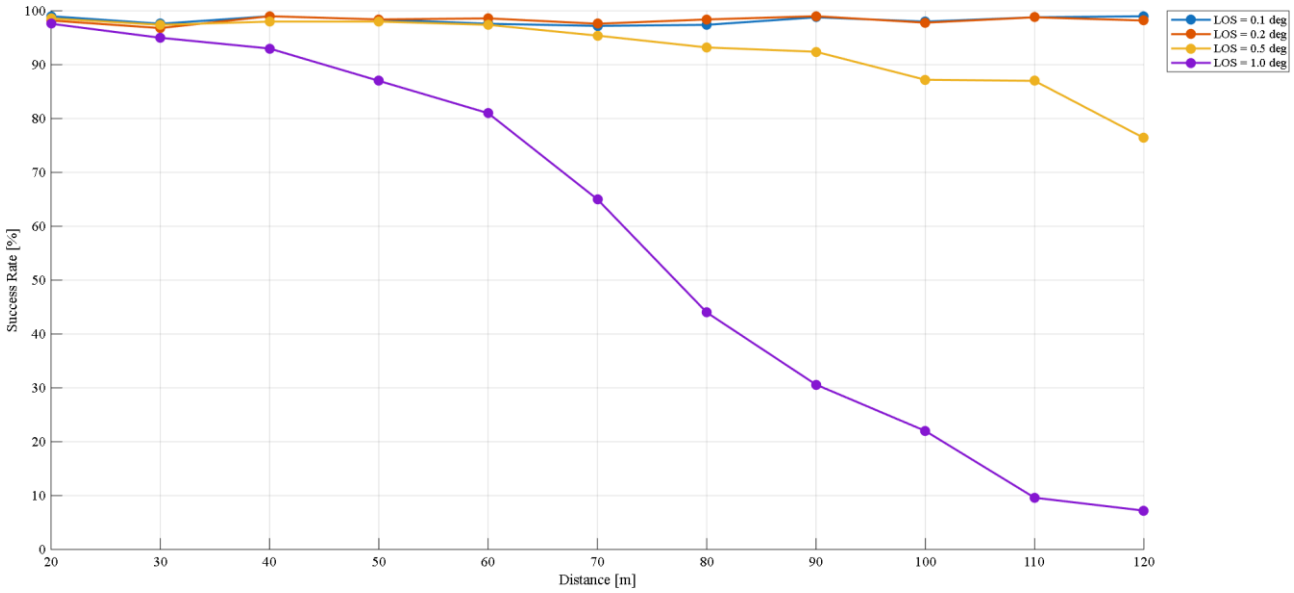

Figura 5.6 – SR vs Distance (NO AR) TDRS

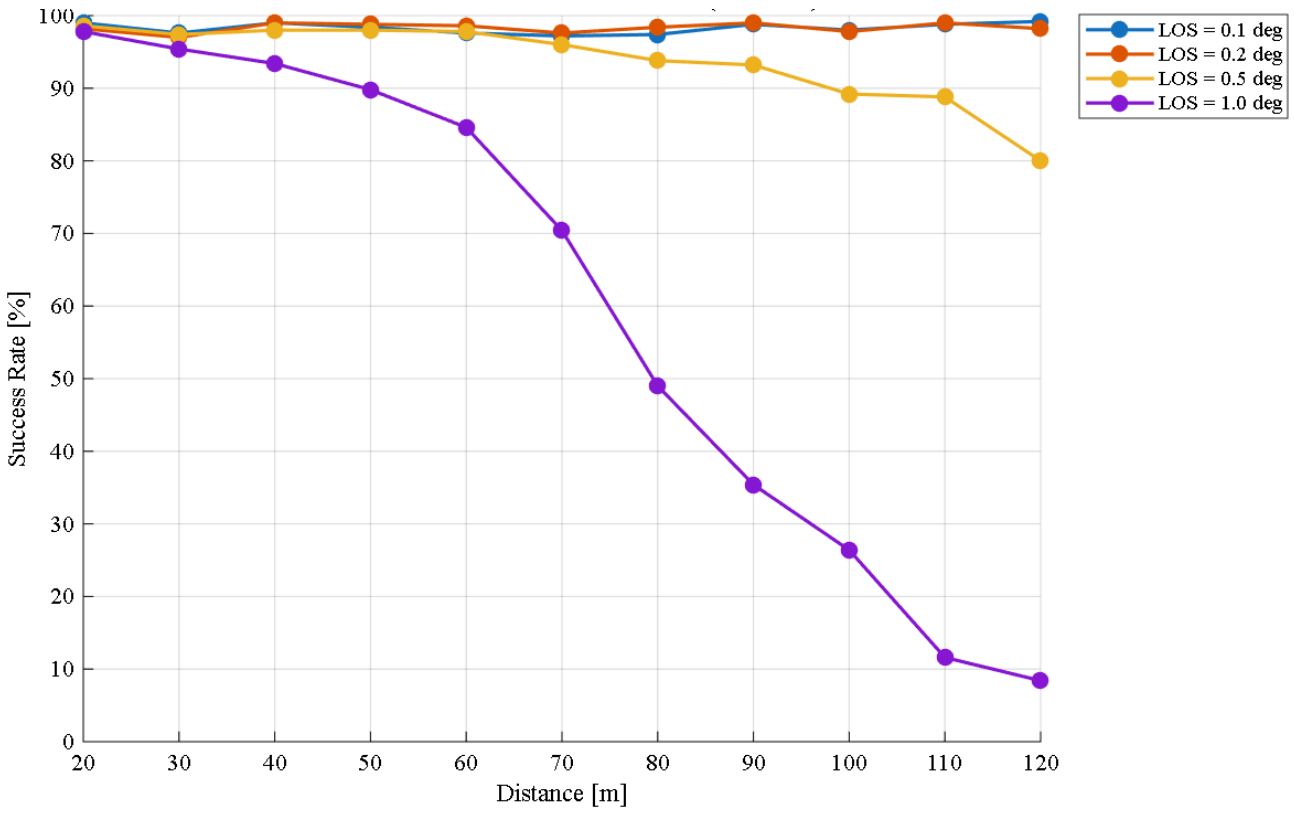

Figura 5.7 – SR vs Distance (with AR) TDRS

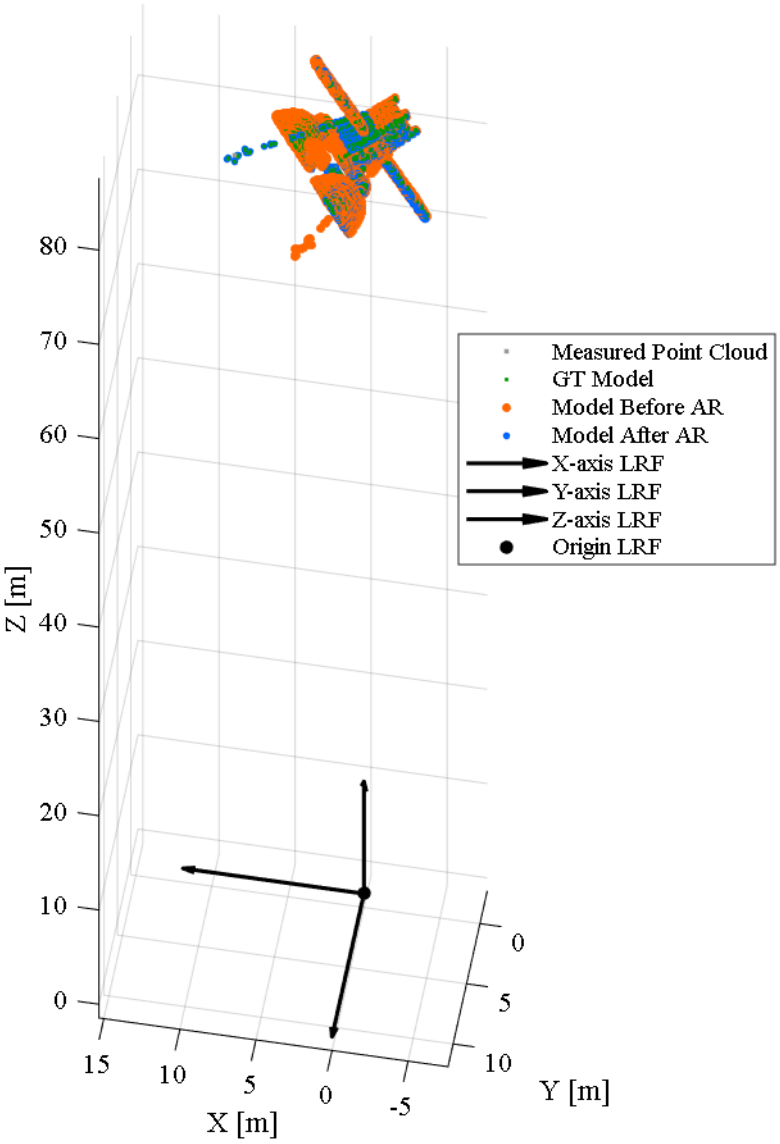

Figura 5.8 – Ambiguity Reduction representation

Performance remains robust at fine resolution, while long-range coarse-resolution configurations define the principal failure regime.

5.2.3 Dawn (X-Axis Symmetry)

Dawn presents more pronounced symmetry characteristics relative to its dominant axis, leading to a lower overall SR ceiling compared to Envisat.

Even at fine resolutions, performance saturation is not as strong, particularly at extended ranges. This indicates that geometric structure plays a critical role beyond mere symmetry classification.

The AR module provides limited improvement in extreme sparsity conditions, where insufficient geometric information prevents reliable discrimination between hypotheses.

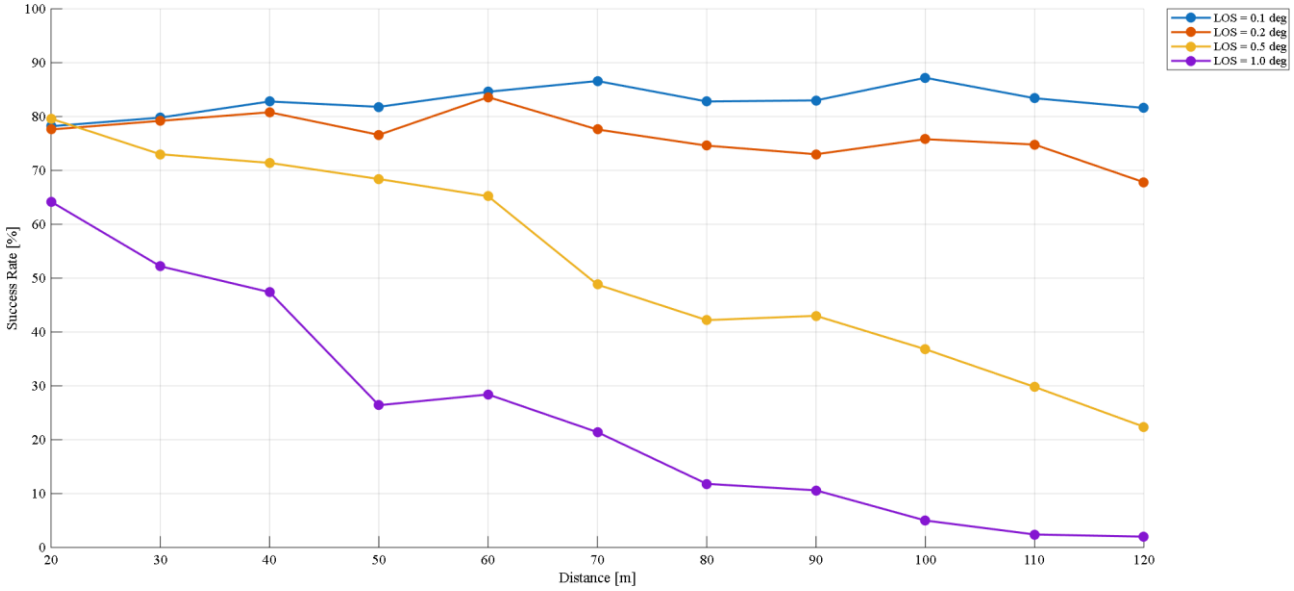

Figura 5.9 – SR vs Distance (NO AR) Dawn

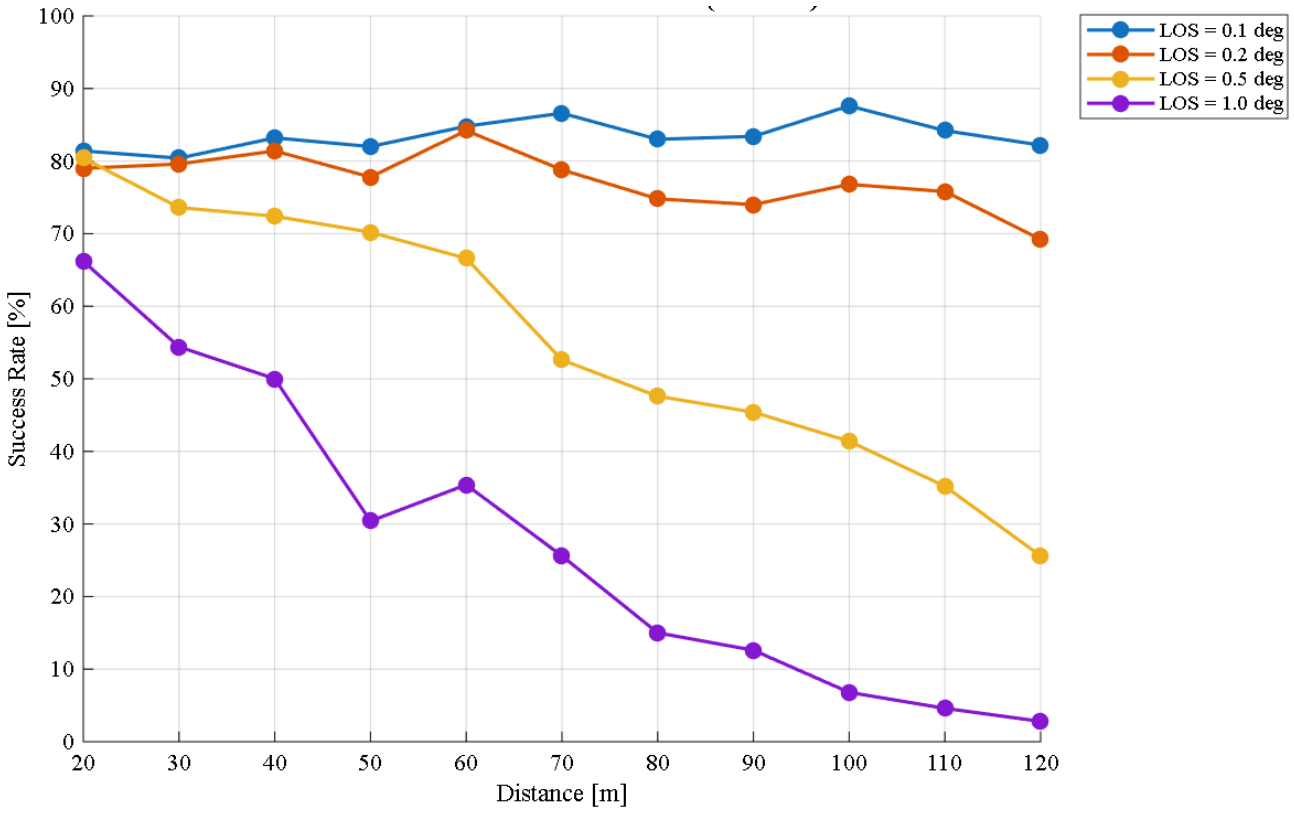

Figura 5.10 – SR vs Distance (with AR) Dawn

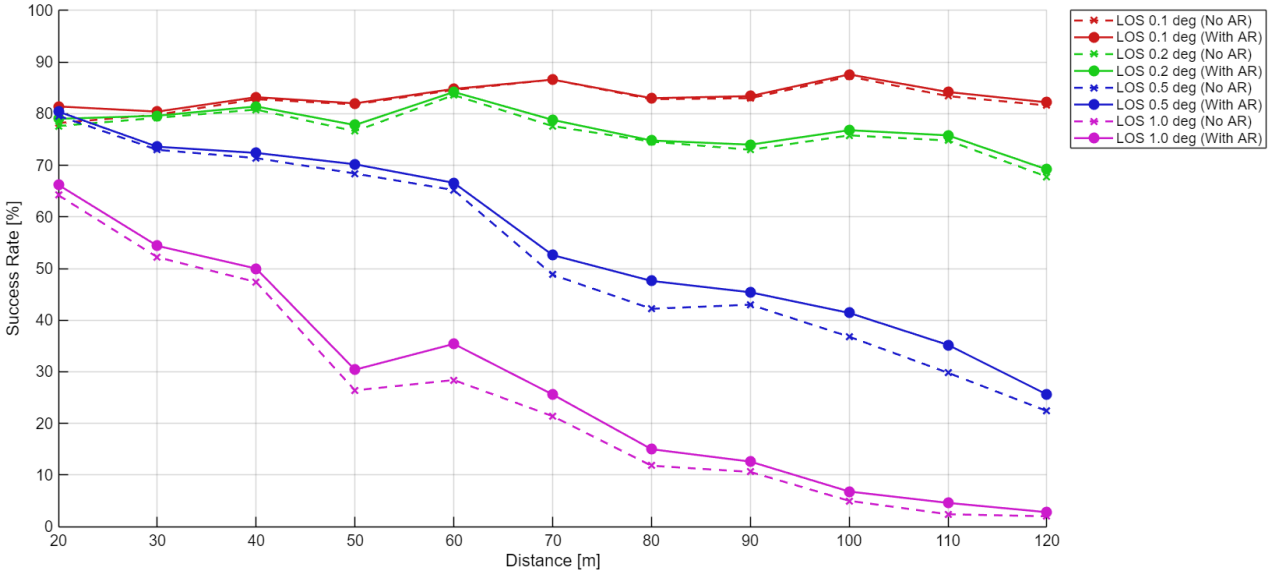

Figura 5.11 – SR Comparison with/without AR for Dawn at all tested sensor resolutions

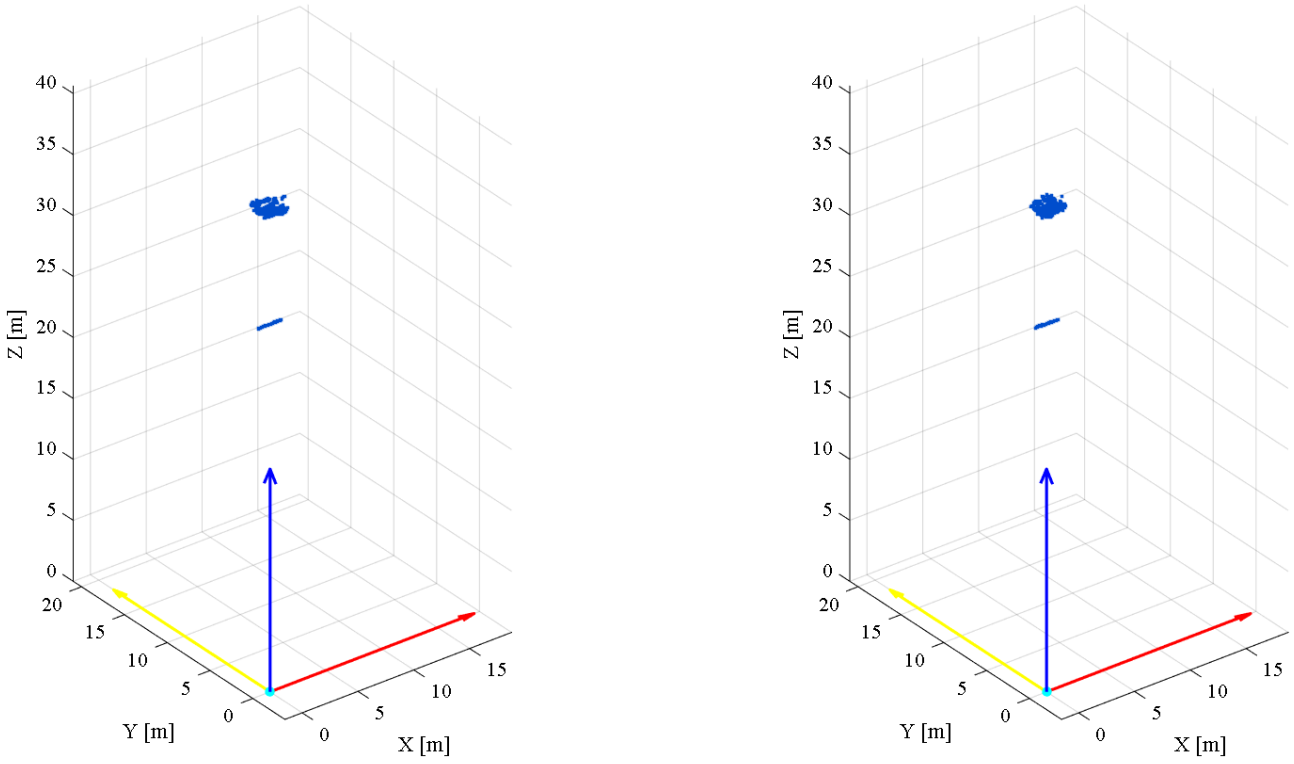

Figura 5.12 – Dawn target viewed at 30m at Pitch angle ~90° and at Yaw angles 0° and 180°, demonstrating pose ambiguities and viewing geometry limitations

The results highlight that for strongly symmetric and sparsely observed geometries, acquisition reliability becomes fundamentally limited by sensing constraints rather than algorithmic design.

5.3 Operational Envelope Summary

The simulation campaign allows identification of three operational regimes:

1. Robust Regime:
   High SR across distances (fine resolution, asymmetric geometry).
2. Transition Regime:
   Performance sensitive to resolution and symmetry (mid-range distances).
3. Failure Regime:
   Long-range + coarse resolution + symmetry → significant SR degradation.

The OBB-TM algorithm demonstrates strong robustness within its intended operational envelope, particularly when sufficient geometric constraints are available. However, extreme sparsity combined with symmetry imposes intrinsic limits to global pose acquisition reliability.

6. Conclusions and Discussion

This work presented a systematic performance analysis of the OBB-TM algorithm for LiDAR-based pose acquisition of non-cooperative spacecraft in lost-in-space conditions. The study evaluated the robustness of the pipeline across multiple target geometries, sensor resolutions, and operational distances through an extensive Monte Carlo campaign.

The results demonstrate that the OBB-TM approach provides a structured and computationally efficient solution to global pose acquisition, effectively reducing the rotational search space from three degrees of freedom to a constrained one-dimensional problem. The combination of PCA-based canonical alignment, 1-DoF template matching, and ICP refinement ensures reliable convergence within a well-defined operational envelope.

From a global perspective, algorithm performance is primarily governed by three coupled factors:

- Point cloud sparsity (distance-dependent),
- Angular resolution of the LiDAR sensor,
- Geometric symmetry of the target.

Performance Envelope

For fine angular resolutions (0.1°–0.2°), the algorithm achieves high Success Rate across a wide range of distances, particularly for asymmetric geometries. As resolution degrades or distance increases, performance transitions into a sensitivity regime characterized by:

- Increased susceptibility to ICP local minima,
- Reduced discriminative power of template matching,
- Amplified centroid bias due to partial field-of-view coverage.

Beyond a critical sparsity threshold, the algorithm enters a failure regime where insufficient geometric information prevents reliable global pose recovery.

Failure Mechanisms

Failure modes observed during the campaign can be categorized into three main classes:

1. *Sparsity-Induced Instability*
   At long range with coarse resolution, reduced surface sampling leads to ill-conditioned covariance estimation in the PCA stage and weak geometric constraints during ICP refinement.
2. *Partial Visibility and Centroid Bias*
   Limited FOV and self-occlusion introduce systematic bias in the point cloud centroid estimation, affecting canonical alignment and degrading coarse initialization.
3. *Symmetry-Induced Ambiguity*
   For targets with rotational symmetry, multiple pose configurations produce nearly equivalent residuals under sparse sampling.
   The Ambiguity Reduction (AR) module mitigates this effect by explicitly testing symmetric hypotheses, yielding measurable improvements for moderately symmetric geometries.

However, in extreme sparsity conditions, ambiguity resolution becomes fundamentally limited by the available measurement information rather than algorithmic refinement.

Operational Implications

The analysis indicates that OBB-TM is particularly suitable for:

- Mid-range acquisition phases,
- Targets with moderate or low symmetry,
- Scenarios with sufficient LiDAR angular resolution.

For highly symmetric targets observed at long range, sensing constraints dominate performance. In such cases, improved sensor resolution, multi-view acquisition, or integration with additional modalities (e.g., vision-based cues) may be required.

Future Developments

Several potential extensions can further enhance the robustness and applicability of the method:

- Adaptive template resolution based on point cloud density,
- Integration with probabilistic scoring metrics instead of purely residual-based selection,
- Fusion with feature-based or learning-assisted initialization strategies,
- Real-time onboard optimization and complexity reduction analysis.

Final Remarks

The presented study confirms that the OBB-TM framework constitutes a viable and structured approach to LiDAR-based pose acquisition of non-cooperative space targets. While performance is inherently bounded by sensing geometry and symmetry properties, the algorithm demonstrates strong robustness within its intended operational envelope and provides a solid foundation for further developments in autonomous relative navigation for OOS and ADR missions.